AMERICAN SOCIETY FOR MICROBIOLOGY | Applied and Environmental Microbiology

Microbial Pathogenesis | Full-Length Text

Autoinducer-2 promotes adherence of *Aeromonas veronii* through facilitating the expression of MSHA type IV pili genes mediated by c-di-GMP

Yi Li,[1,2] Shuo Han,[1,2] Yuqi Wang,[1,2] Mengyuan Qin,[1,2] Chengjin Lu,[1,2] Yingke Ma,[1] Wenqing Yang,[1] Jiajia Liu,[1] Xiaohua Xia,[1] Hailei Wang[1,2,3]

AUTHOR AFFILIATIONS See affiliation list on p. 17.

ABSTRACT *Aeromonas veronii*. a ubiquitous of zoonotic disease pathogen, depends on adhesion as the crucial way to colonize the gastrointestinal tract of humans and animals, which further causes severe gastrointestinal diseases and parenteral infections. However, the adherence mechanism of *A. veronii* has not been fully characterized. Therefore, we investigate the effect of autoinducer-2 (AI-2) on adherence of *A. veronii* through facilitating the expression of mannose-sensitive hemagglutinin (MSHA) type IV pili genes mediated by cyclic diguanosine monophosphate (c-di-GMP). The deficiency of AI-2 significantly lowered the adherence of *A. veronii* to erythrocytes and intestinal mucus, and the complement of AI-2 could increase its adherence ability. The deficiency of AI-2 only limited the formation of pili, instead of outer-membrane proteins and lipopolysaccharide, through reducing the expression levels of MSHA type IV pili genes due to the decline of c-di-GMP. The addition of guanosine triphosphate (GTP) could increase the content of c-di-GMP and the expression of MSHA type IV pili genes, and further promote adherence of *A. veronii*. Therefore, this study reveals, for the first time, adherence mediated by c-di-GMP with MshE as the c-di-GMP receptor is positively regulated by AI-2 in *A. veronii*, which increases the understanding of colonization strategy of pathogen and may facilitate control of *A. veronii* infection to host.

IMPORTANCE *Aeromonas veronii* can adhere to host cells through different adherence factors including outer-membrane proteins (OMPs), lipopolysaccharide (LPS), and pili, but its adherence mechanisms are still unclear. Here, we evaluated the effect of autoinducer-2 (AI-2) on adherence of *A. veronii* and its regulation mechanism. After determination of the promotion effect of AI-2 on adherence, we investigated which adherence factor was regulated by AI-2, and the results show that AI-2 only limits the formation of pili. Among the four distinct pili systems, only the mannose-sensitive hemagglutinin (MSHA) type IV pili genes were significantly downregulated after deficiency of AI-2. MshE, an ATPase belonged to MSHA type IV pilin, was confirmed as c-di-GMP receptor, that can bind with c-di-GMP which is positively regulated by AI-2, and the increase of c-di-GMP can promote the expression of MSHA type IV pili genes and adherence of *A. veronii*. Therefore, this study confirms that c-di-GMP positively regulated by AI-2 binds with MshE, then increases the expression of MSHA pili genes, finally promoting adherence of *A. veronii*, suggesting a multilevel positive regulatory adhesion mechanism that is responsible for *A. veronii* adherence.

KEYWORDS *Aeromonas veronii*, autoinducer-2, adherence, MSHA type IV pili, c-di-GMP

Bacteria of the genus *Aeromonas*, the Gram-negative pathogens, are found ubiquitously in the environment and host (1), which can colonize the gastrointestinal tract

Editor Charles M. Dozois, INRS Armand-Frappier Sante Biotechnologie Research Centre, Laval, Quebec, Canada

Address correspondence to Xiaohua Xia, xxhlpf@163.com, or Hailei Wang, whl@htu.cn.

Yi Li and Shuo Han contributed equally to this article. Author order was determined by the degree of contribution to the manuscript.

The authors declare no conflict of interest.

See the funding table on p. 17.

Received 17 May 2023
Accepted 19 September 2023

Published 30 October 2023

[This article was published on 30 October 2023 with an incorrect figure citation in the second paragraph of the Results section. The citation was adjusted in the current version, posted on 7 November 2023.]

of humans and animals, thereby causing severe wound infections, internal hemorrhaging, and gastroenteritis (2). *Aeromonas veronii*, 1 of the 31 valid species belonged to the genus *Aeromonas* (https://lpsn.dsmz.de/genus/aeromonas), is the main pathogen that responsible for human clinical cases (3). The most common disease caused by *A. veronii* is gastroenteritis, especially in infants and young children who experience varying degrees of diarrhea after infection (4). The infection of *A. veronii* depends on its colonization in the host gastrointestinal tract (5), and prevention of *A. veronii* colonization can effectively alleviate the harm it causes to human.

Adhesion is a crucial step for pathogens to colonize and infect the host, which can promote pathogens to adhere to the surface of the host mucosa (6). *A. veronii* possesses a variety of adhesins on the cell surface that contribute to its adherence to host cells. Outer-membrane proteins (OMPs) have been confirmed as the adhesins in *A. veronii* that a decreased adherence of *A. veronii* to HeLa cells after pre-incubation with anti-Omp48 anti-serum (7). Previous studies have reported that lipopolysaccharide (LPS) has been associated with adherence to HEp-2 cells by *A. hydrophila* (8). In addition, the type IV bundle-forming pili (Bfp) such as the mannose-sensitive hemagglutinin (MSHA) type pili, the firstly isolated from *A. veronii* (9), are among the most important adhesins for *A. veronii* adherence to host cells (10). Despite the fact that we already have a clear understanding of the adhesins in *A. veronii*, little is known about the adherence mechanisms of *A. veronii*.

Previous research has focused on the effect of cyclic diguanosine monophosphate (c-di-GMP), a bacterial intracellular second messenger, on the adherence of *A. veronii*, which confirmed that the overexpression of the GGDEF domain protein AdrA that is responsible for the synthesis of c-di-GMP enhances the adhesion to aquatic plant duckweed and amoeba surfaces (11). c-di-GMP has been thought of as a key factor in regulating adherence of *A. veronii*, but the c-di-GMP receptor as the c-di-GMP binding protein is still unclear in *A. veronii*, as well as the metabolic regulation pathways of c-di-GMP. The synthesis of c-di-GMP has been reported to be negatively regulated by HapR (12), the LuxR homolog as a LuxS/AI-2 quorum-sensing (QS) master regulator. LuxS/AI-2 system, a bacterial cell-to-cell communication depending on AI-2 as autoinducer that regulates gene expression, has not been fully characterized its regulation role in the synthesis of c-di-GMP in *A. veronii* and its adherence.

In this study, we investigated the regulation effect of AI-2 on adherence of *A. veronii*, as well as the expression of MSHA type IV pili genes mediated by c-di-GMP. Our results show that the deficiency of AI-2 promotes the expression of *hapR* in *A. veronii*, and lowers the content of c-di-GMP; the decline of c-di-GMP limits the expression of *mshE*, as well as MSHA pili genes. The declined expression of MSHA pili genes finally affects the formation of pili and causes a decrease in adhesion. This study aims to reveal an AI-2 regulated adherence strategy mediated by c-di-GMP, which will contribute to inhibiting the adhesion of pathogen and its control.

RESULTS

Determination of the gene, *luxS*, that responsible for AI-2 synthesis

The synthesis of AI-2 in bacteria depends on a two-step enzymatic catalysis by the Pfs and LuxS enzymes with S-adenosyl-homocysteine (SAH) as substrate (13), and the LuxS enzyme, which is encoded by gene *luxS*, is responsible for the last enzymatic step of AI-2 synthesis (Fig. 1A). Therefore, the construction of AI-2 deficient strain was performed by deletion of gene *luxS* in the genome of *A. veronii* Z12 according to the schematic representation in Fig. 1B, and the complement of AI-2 deficient strain Z12Δ*luxS* was achieved by adding exogenous synthesized AI-2 to the AI-2 deficient strain. The confirmation of *luxS* deletion by PCR amplification showed that the electrophoresis band of the PCR product with primers F1, R1 in wild strain Z12 was higher than 2,000 bp (Fig. 1C), and exhibited an electrophoretic band around 450 bp with primers F2, R2 (Fig. 1D). However, PCR product in strain Z12Δ*luxS* exhibited an electrophoretic band around 2,000 bp with primers F1, R1, which was lower than that of wild strain

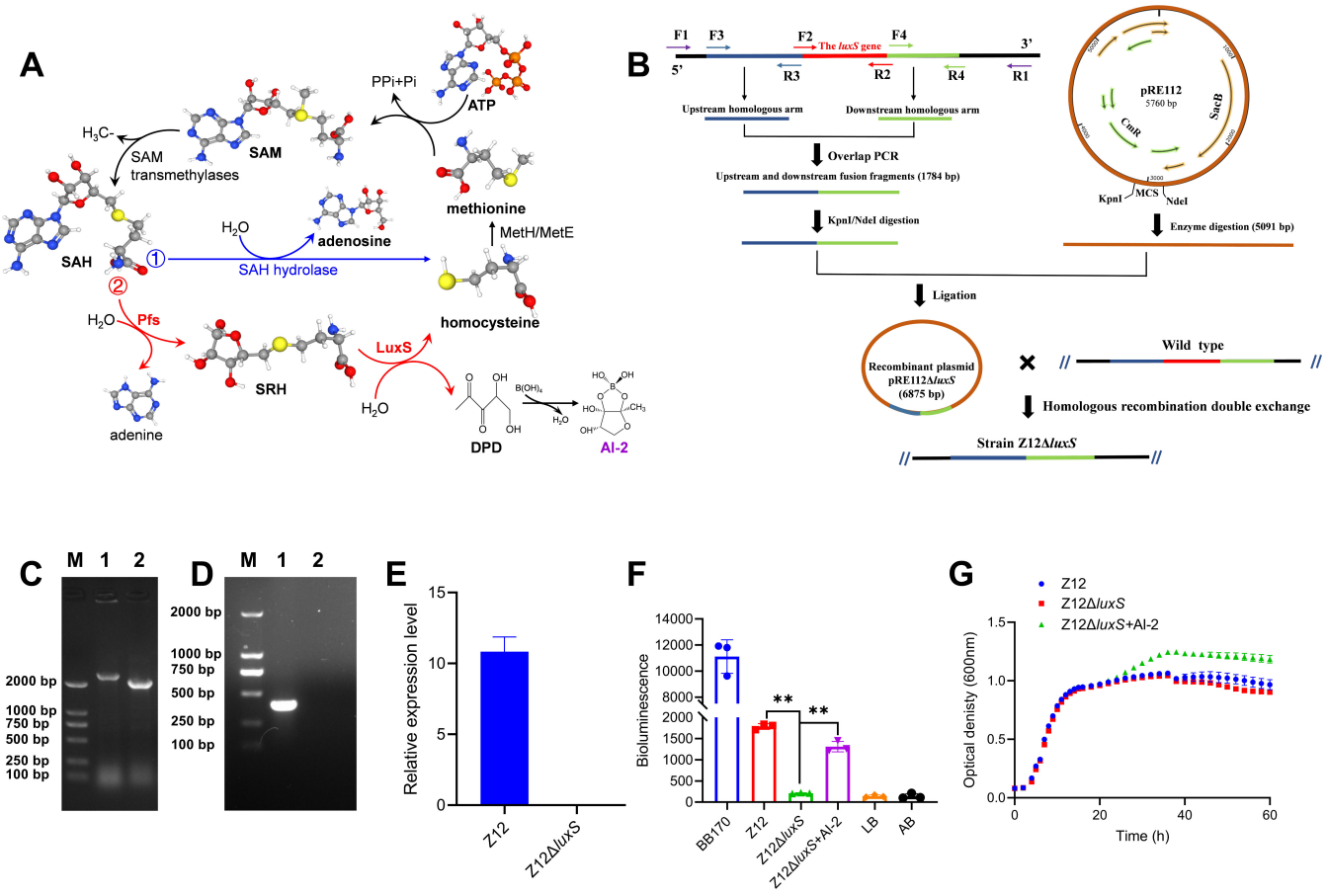

FIG 1 The construction of AI-2 deficient strain and complement. (A) AI-2 biosynthesis pathway. SAM, S-adenosyl-methionine; SAH, S-adenosyl-homocysteine; SRH, S-ribosyl-homocysteine; DPD, 4,5-dihydroxyl-2,3-pentanedione; AI-2, autoinducer-2. (B) Schematic representation of the *luxS* gene deletion. (C) The electrophoresis bands of the PCR products with primers F1 and R1. M, marker; Lane 1, the wild strain Z12; Line 2, the mutation strain Z12Δ*luxS*. (D) The electrophoresis bands of the PCR products with primers F2 and R2. M, marker; Lane 1, the wild strain Z12; Line 2, the mutation strain Z12Δ*luxS*. (E) The relative expression level of gene *luxS* in strains Z12 and Z12Δ*luxS*. (F) AI-2 levels which are detected by luminescence of *V. harveyi* BB170 with addition of cell-free culture of strains Z12, Z12Δ*luxS*, and Z12Δ*luxS*+AI-2. (G) Bacterial growth levels of strains Z12, Z12Δ*luxS*, and Z12Δ*luxS*+AI-2. Data are presented as mean ± SD. ** represents a statistically significant difference of $P < 0.01$.

Z12, but exhibited no electrophoretic band with primers F2, R2. Meanwhile, the relative expression level of gene *luxS* in wild strain Z12 and strain Z12Δ*luxS* was determined by real-time quantitative PCR (RT-qPCR), the result showed that gene *luxS* in strain Z12 could exhibit a high expression level, but no transcription was detected in the mutant strain Z12Δ*luxS* (Fig. 1E), suggesting that gene *luxS* was successfully implemented to be deleted from the genome of strain Z12. To further determine whether gene *luxS* responsible for AI-2 synthesis, as well as the successful construction of AI-2 deficient strain and complement, *V. harveyi* BB170 was used as reporter strain to measure its bioluminescence in response to exogenous AI-2 content, thus characterizing the AI-2 level in strain Z12, strain Z12Δ*luxS*, as well as strain Z12Δ*luxS* with adding exogenous AI-2 (Z12Δ*luxS* + AI-2). As shown in Fig. 1F, the bioluminescence levels of strain BB170 with addition of Z12 cell-free culture and Z12Δ*luxS* + AI-2 cell-free culture were significantly ($P < 0.01$) higher than that of Z12Δ*luxS* cell-free culture, and the bioluminescence levels of strain BB170 with addition of Z12Δ*luxS* cell-free culture exhibited no significant difference with that of negative control, which indicated that the *luxS* mutation strain Z12Δ*luxS* lost the ability to produce AI-2, and the exogenous synthesized AI-2 can be recognized as the complement to strain Z12Δ*luxS*, we have successfully obtained AI-2 deficient strain Z12Δ*luxS* and complement (Z12Δ*luxS* + AI-2). The bacterial growth

conditions were also determined and the results showed that there were no differences in the bacterial growth between different groups within the initial 30 h. However, the bacterial concentration was higher in the Z12Δ*luxS*+AI-2 group than that in the other groups in the subsequent cultivation process. And ultimately, strain Z12 also showed a higher bacterial concentration than the Z12Δ*luxS* group (Fig. 1G).

AI-2 promotes adhesion of *A. veronii* to erythrocytes and intestinal mucus

To investigate the effect of AI-2 on adhesion of *A. veronii*, we compared the adhesion ability of strains Z12 and Z12Δ*luxS* to erythrocytes and intestinal mucus of loach, respectively. As shown in Fig. 2A, the surface of erythrocytes was adhered with more FITC-labeled bacterial cells of strain Z12, but fewer FITC-labeled bacterial cells of strain Z12Δ*luxS* were observed to adhere to the surface of erythrocytes. However, the addition of exogenous AI-2 could promote adhesion of strain Z12Δ*luxS* to erythrocytes. We further performed statistical analysis on the number of bacterial cells adhering to erythrocytes, and the results showed that the number of bacterial cells adhering to

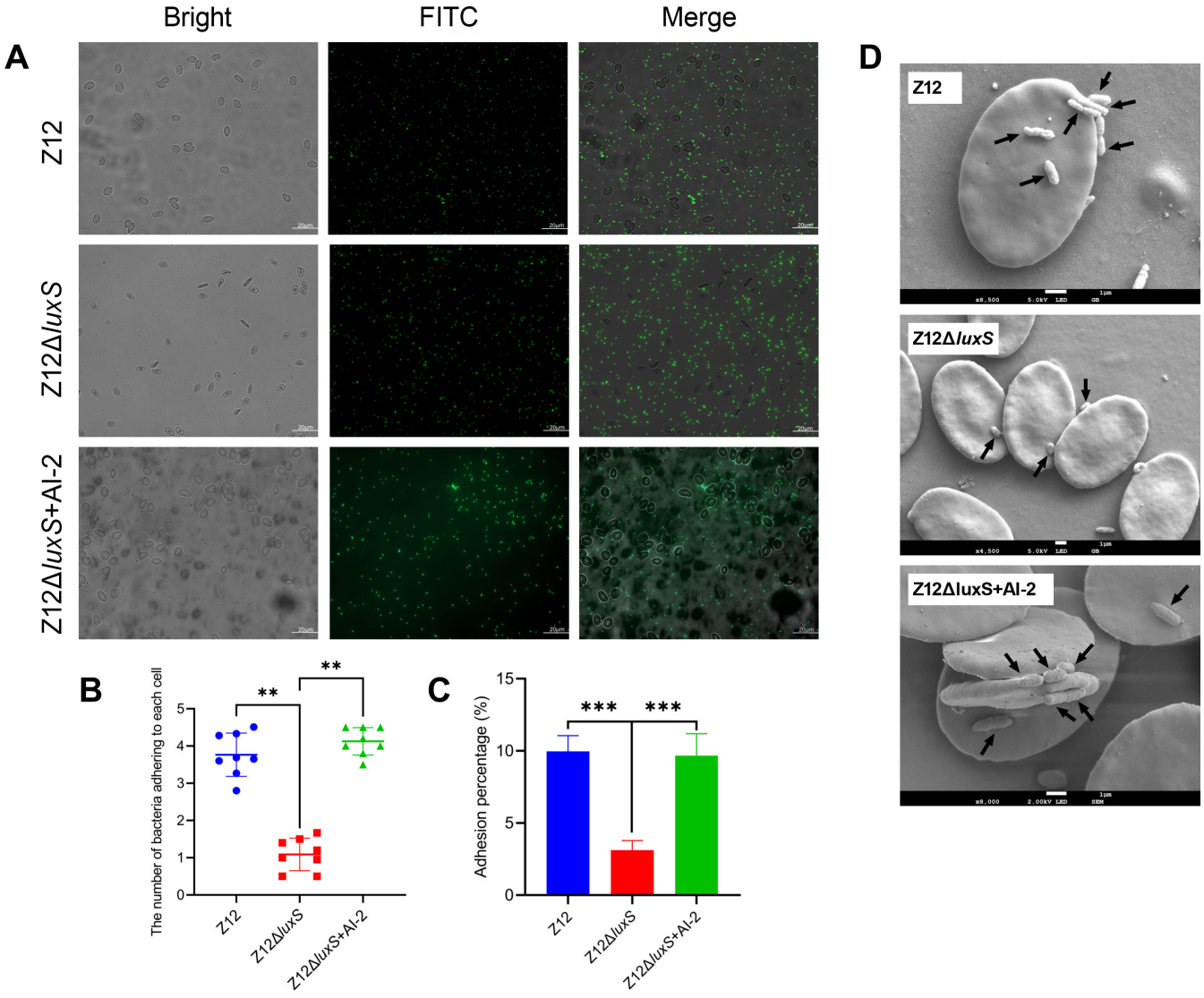

FIG 2 The effect of AI-2 on adherence of *A. veronii* to erythrocytes. (A) The adherence of FITC-labeled bacterial cells to erythrocytes. Scale bars represent 20 µm. (B) The number of bacterial cells adhering to each erythrocyte. (C) Adhesion percentage of strains Z12, Z12Δ*luxS*, and Z12Δ*luxS* + AI-2. (D) Scanning electron microscopy analysis of adherence by strains Z12, Z12Δ*luxS*, and Z12Δ*luxS* + AI-2 to erythrocytes. Arrows represent where bacterial cells adhering to erythrocyte. Data are presented as mean ± SD. ** represents a statistically significant difference of $P < 0.01$. *** represents a statistically significant difference of $P < 0.001$.

erythrocytes was about fourfold higher in the Z12 group and Z12Δ*luxS* + AI-2 group than that in the Z12Δ*luxS* group (Fig. 2B). Strain Z12Δ*luxS* exhibited a significant (P < 0.01) lower adhesion ability compared with strain Z12 or the addition of exogenous AI-2 (Fig. 2C). To better observe the adhesion effect of bacteria on erythrocytes, scanning electron microscopy analysis in the Z12 group, Z12Δ*luxS* group, and Z12Δ*luxS* + AI-2 group was determined. Results showed that most of the erythrocytes were adhered with more bacterial cells in the Z12 group and Z12Δ*luxS* + AI-2 group, but erythrocytes in the Z12Δ*luxS* group were not adhered with bacterial cells or less bacterial cells (Fig. 2D). Altogether, these results suggest that AI-2 can improve the adhesion ability of *A. veronii* to erythrocytes. *A. veronii*, a pathogen that can colonize the intestine, was further performed to investigate whether AI-2 can improve the adhesion ability of *A. veronii* to intestinal mucus (Fig. S1). The results showed that the number of FITC-labeled bacterial cells adhering to intestinal mucus in the Z12 group was significantly (P < 0.05) higher than that in the Z12Δ*luxS* group (Fig. S1A through C), strain Z12Δ*luxS* exhibited a significant (P < 0.01) lower adhesion ability to intestinal mucus compared with strain Z12 (Fig. S1C), which indicated that AI-2 can also promote the adhesion ability of *A. veronii* to intestinal mucus.

AI-2 can regulate the formation of pili

To further determine how AI-2 promotes the adhesion of *A. veronii*, we investigated three major adherence factors including OMPs, LPS, and pili between strains Z12 and Z12Δ*luxS*. The results showed that there were no obvious differences in the contents of OMPs and LPS between strains Z12 and Z12Δ*luxS* (Fig. 3A through D). The forming abilities of bacterial pili in strains Z12 and Z12Δ*luxS* were determined by transmission electron microscopy analysis, which showed that strain Z12 formed multiple pili around the bacterial cells (Fig. 3E and F), but strain Z12Δ*luxS* lost the ability to form pili and could not be observed pili around the bacterial cells (Fig. 3G and H). Based on these data, we confirm that AI-2 can promote the formation of pili, which may be involved in the adherence of *A. veronii*.

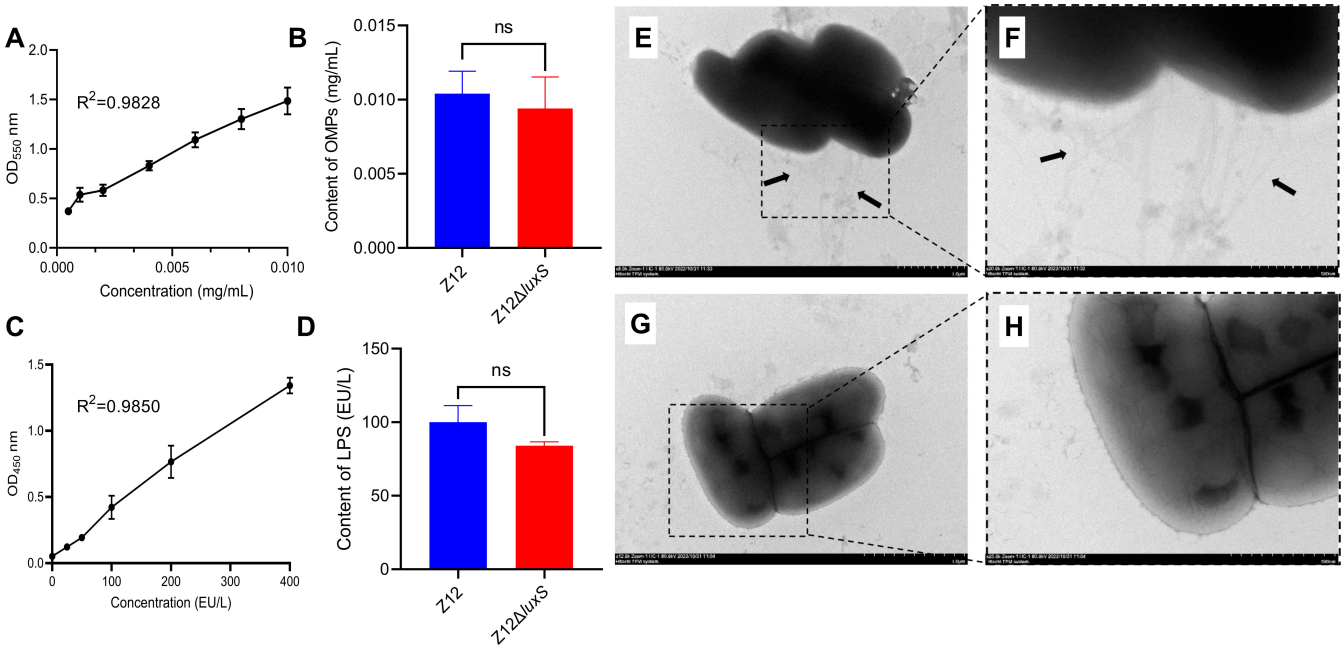

FIG 3 Adhesins including OMPs, LPS, and pili of strains Z12 and Z12Δ*luxS*. (A and B) The contents of OMPs. (C and D) The contents of LPS. (E and F) Transmission electron microscopy analysis of Z12 cells that arrows represent pili of strain Z12. (G and H) Transmission electron microscopy analysis of Z12Δ*luxS* cells. Data are presented as mean ± SD. ns represents no statistically significant difference.

AI-2 facilitates the expression of the MSHA type IV pili genes

A variety of pili have been found in the surface of *A. veronii*, which can allow bacterial cells to adhere to host. It is generally accepted that *Aeromonas* spp. possess two distinct pili types including short-rigid (S/R) called type I pili and long-wavy (L/W) called type IV pili (14). Based on our previous genome analysis of *A. veronii* Z12 (15), two type IV pili gene families, including Tap homologous pili (*pil* gene family) and MSHA pili family, were found in the genome of *A. veronii* Z12, as well as *csg* gene family responsible for curli production and *fim* gene family responsible for fimbrial protein (Table S1). To further determine which pili system is regulated by AI-2 and thus can affect the formation of pili, the relative expression levels of the pili genes including *csg* gene family, *fim* gene family, *pil* gene family, and MSHA pili family between strains Z12 and Z12Δ*luxS* were investigated. As shown in Fig. 4A, compared to those in the wild strain Z12, the expression levels of the *csg* gene family except *csgE* were upregulated ($P < 0.01$) in mutant strain Z12Δ*luxS*. The expression levels of the *fim* gene family showed a similar trend to that of the *csg* gene family, with all genes except for the *fimTV* genes upregulated in mutant strain Z12Δ*luxS*, which were significantly ($P < 0.01$) higher than of wild strain Z12 (Fig. 4B). The *pil* gene family contained the most pili genes, with 24 of genes, the expression levels of these genes between strains Z12 and Z12Δ*luxS* were determined. The results showed that the expression levels of 20 genes were upregulated to varying degrees in mutant strain Z12Δ*luxS*, with only 4 genes having lower expression levels in strain Z12Δ*luxS* than that in the wild strain Z12 (Fig. 4C). Different from the expression levels of the other three gene families between strains Z12 and Z12Δ*luxS*, the expression levels of 11 out of 15 MSHA genes in mutant strain Z12Δ*luxS* were lower than those in wild strain Z12 (Fig. 4D). Altogether, these results show that deficiency of AI-2 inhibits the expression levels of MSHA pili family, but promoting the expression levels of *csg* gene family, *fim* gene family, and *pil* gene family. Meanwhile, the deficiency of AI-2 limits the formation of pili. Therefore, MSHA pili family, which was regulated by AI-2, plays a key role in pili formation of *A. veronii* Z12.

AI-2 promotes the synthesis of c-di-GMP

Since AI-2 can promote pili formation of *A. veronii* Z12 through facilitating the expression of MSHA pili genes, the pathway by which AI-2 affects the expression of MSHA pili genes deserves further exploration. Among the MSHA pili family, ATPase responsible for pilus polymerization, functions to retract the pilus from the cell surface, which plays a central role in forming pili and adhering (16). Based on Non-Redundant Protein Sequence Database of the genome analysis, MshE, which was encoded by *mshE*, has been characterized as the MSHA polymerization ATPase. Meanwhile, MshE, as a high-affinity c-di-GMP receptor (17), can interact with c-di-GMP to perform its functions. Therefore, we were wondering whether AI-2 regulated *mshE* gene expression through influencing the synthesis of c-di-GMP. To verify whether MshE can interact with c-di-GMP, the CD spectrum of purified MshE protein and different concentrations of c-di-GMP was performed. As shown in Fig. 5A, the interaction between MshE and c-di-GMP causes obvious changes in ellipticities of the far-UV and near-UV CD, c-di-GMP-bound MshE induced ellipticities decreased with increasing c-di-GMP concentrations at around 220 nm, and the CD peak at around 260 nm increased with increasing c-di-GMP concentration. C-di-GMP can interact with MshE in a dose-dependent manner, causing significant changes in the secondary and tertiary structures of MshE, thereby affecting its function. Also, the contents of c-di-GMP in strains Z12 and Z12Δ*luxS* were measured based on HPLC. The HPLC absorption peak height of c-di-GMP in strain Z12Δ*luxS* was lower than that of strain Z12 (Fig. 5B and C), and the content of c-di-GMP was calculated by the standard curve of absorption peak height and concentration of c-di-GMP standard, and the results showed that the content of c-di-GMP in mutant strain Z12Δ*luxS* was significantly ($P < 0.01$) lower than that in wild strain Z12 (Fig. 5D). And we further investigated the possible reason for the decrease in c-di-GMP content caused by the absence of AI-2. Previous studies have demonstrated that HapR, the LuxR homolog

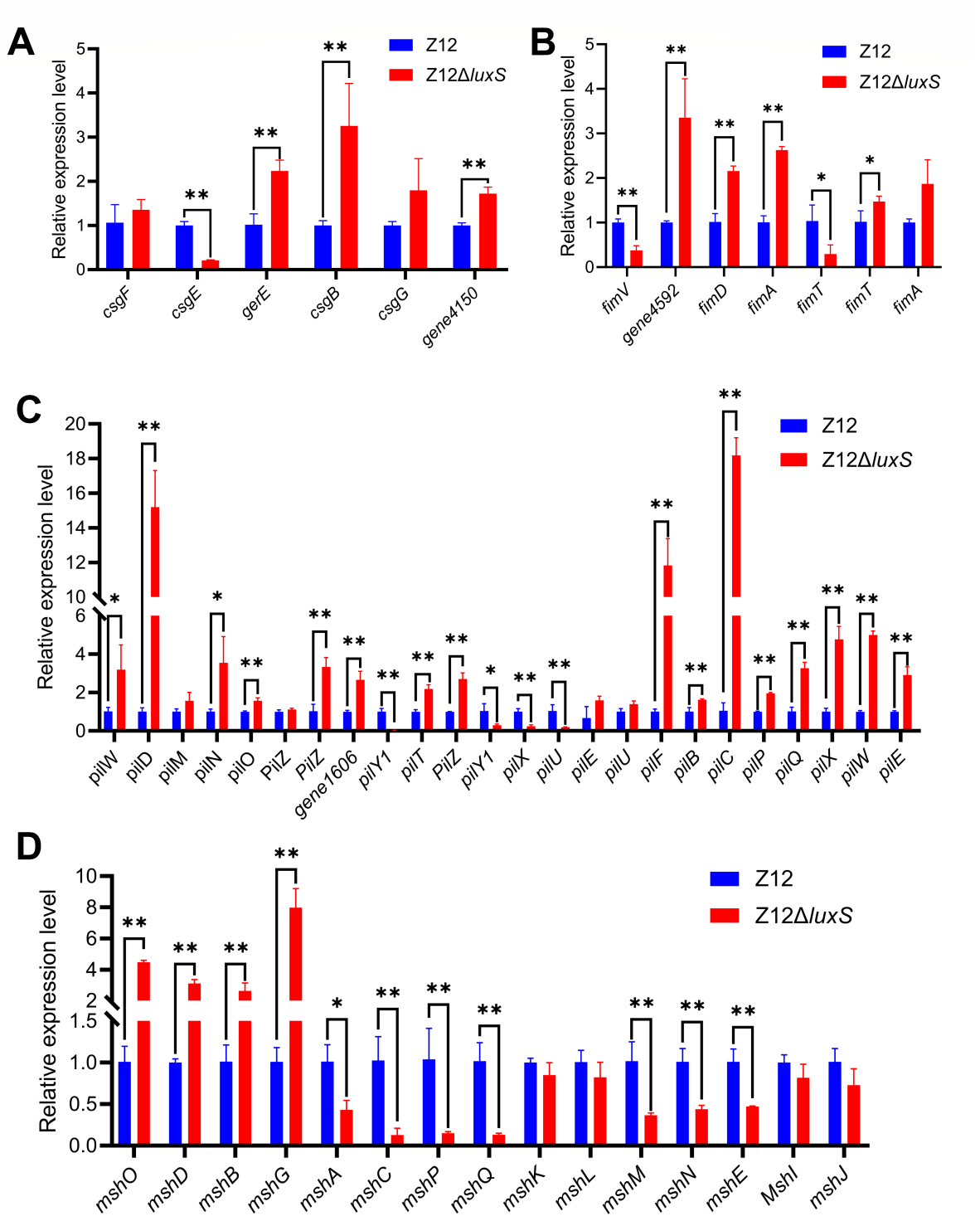

FIG 4 The relative expression levels of pili genes in strains Z12 and Z12Δ*luxS*. (A) The relative expression level of *csg* gene family. (B) The relative expression level of *fim* gene family. (C) The relative expression level of *pil* gene family. (D) The relative expression level of MSHA pili family. Data are presented as mean ± SD. * represents a statistically significant difference of $P < 0.05$. ** represents a statistically significant difference of $P < 0.01$.

as a LuxS/AI-2 quorum-sensing master regulator that is responsible for responding to AI-2 and regulating downstream target genes (18), can lower the intracellular level of c-di-GMP (12). Therefore, we investigated the relative expression level of *hapR* between strains Z12 and Z12Δ*luxS*, and the results showed that the expression level of *hapR*

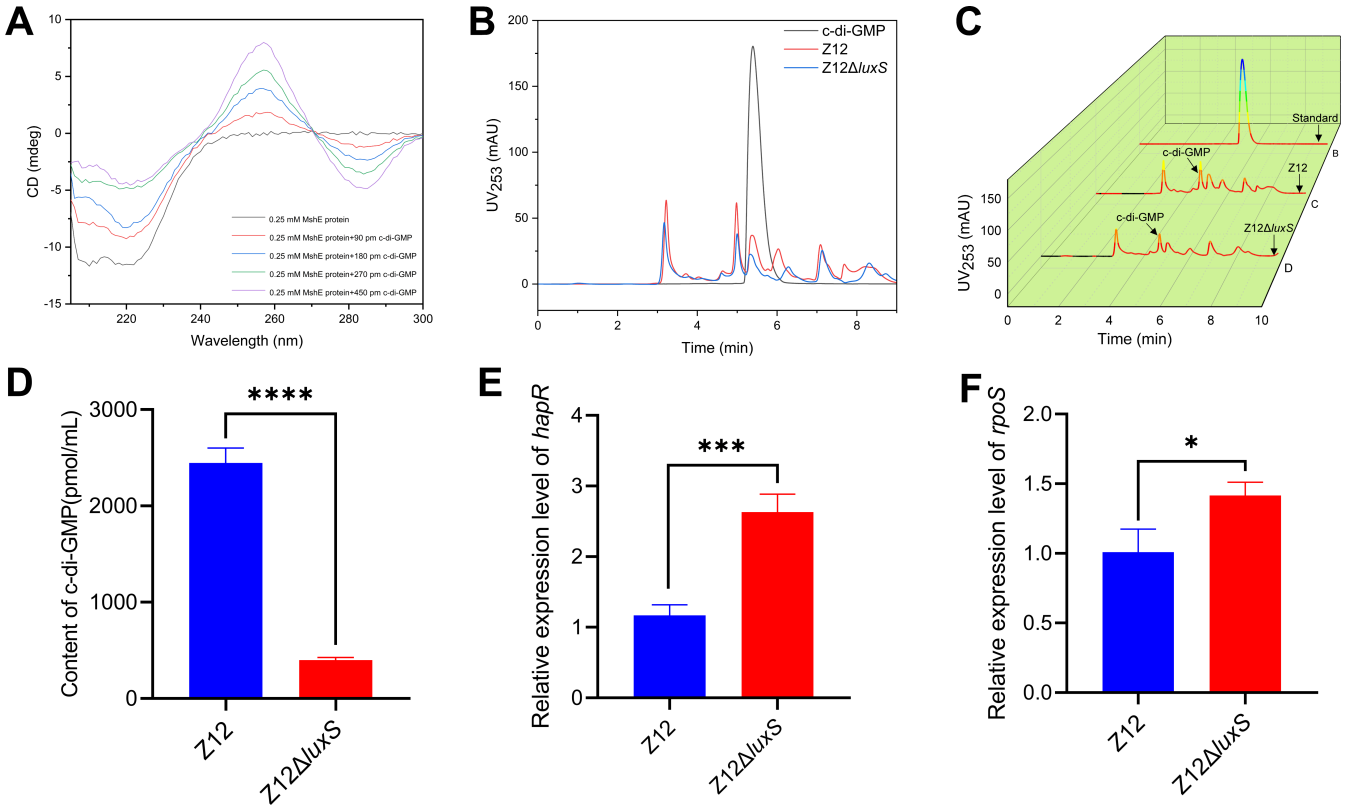

FIG 5 The effect of AI-2 on synthesis of c-di-GMP. (A) CD spectra of MshE with different concentrations of c-di-GMP. (B) HPLC spectra of c-di-GMP in strains Z12 and Z12Δ*luxS*. (C) HPLC 3D spectra of c-di-GMP in strains Z12 and Z12Δ*luxS*. (D) The contents of c-di-GMP in strains Z12 and Z12Δ*luxS*. (E) The relative expression level of *hapR*. (F) The relative expression level of *rpoS*. Data are presented as mean ± SD. * represents a statistically significant difference of $P < 0.05$. *** represents a statistically significant difference of $P < 0.001$. **** represents a statistically significant difference of $P < 0.0001$.

in strain Z12 was significantly ($P < 0.01$) lower than that in strain Z12Δ*luxS* (Fig. 5E), which indicated that the high expression level of *hapR* in strain Z12Δ*luxS* may cause the decrease of c-di-GMP. However, the high expression level of *hapR* in AI-2 deficient strain is not consistent with other reports (19), which confirmed that the absence of AI-2 caused phosphorylated LuxO to activate Qrr sRNA, thereby activating translation of the low-cell-density master regulator aphA, but inhibiting the master regulator HapR. To reveal the reason for high expression level of *hapR* in strain Z12Δ*luxS*, we investigated the relative expression level of *rpoS* between strain Z12 and Z12Δ*luxS*, which showed that the expression level of *rpoS* in strain Z12 was significantly ($P < 0.05$) lower than that in strain Z12Δ*luxS* (Fig. 5F). The sigma factor RpoS, which was encoded by *rpoS*, has been evidenced that can significantly stabilized mRNA of LuxR homologous protein VanT and induced its expression (20). Therefore, the high expression level of *rpoS* may promote the expression of *hapR*, thereby causing the decline of c-di-GMP. Altogether, these results suggested that the deficiency of AI-2 promotes the expression of *rpoS*, may induce high expression of *hapR*, thereby limiting the synthesis of c-di-GMP, and further affecting the normal functioning of MshE.

C-di-GMP promotes the expression of MSHA type IV pili genes

Generation of c-di-GMP depends on the diguanylate cyclases (DGCs) containing GGDEF domain with two molecules of GTP as specific substrate (Fig. S2). To further evaluate the synthesis level of c-di-GMP in strain Z12 and its effect on expression levels of MSHA type IV pili genes, we investigated the addition of 1 mM GTP on the expression levels of genes encoding DGC proteins. Based on genome analysis of strain Z12, DgcB and TpbB

proteins, which were encoded by gene *dgcB* and *tpbB*, contained GGDEF domains. We compared the relative expression levels of *dgcB* and *tpbB* in strains Z12 and Z12Δ*luxS* with or without adding GTP, the results showed that the expression levels of *dgcB* and *tpbB* in strain Z12 were significantly higher than that in strain Z12Δ*luxS* (Fig. 6A), this also explains why the content of c-di-GMP in the mutant strain Z12Δ*luxS* is low. The expression levels of *dgcB* and *tpbB* were significantly ($P < 0.01$) upregulated in strain Z12 with adding exogenous GTP (Fig. 6A), suggesting that GTP can be added as specific substrate to promote the expression of genes encoding DGC proteins. The high expression levels of genes encoding DGC proteins may contribute to the synthesis of c-di-GMP; therefore, we further investigate the effect of GTP on the c-di-GMP content in strain Z12. The HPLC absorption peak height of c-di-GMP in strain Z12 with adding exogenous GTP was obviously higher than that of strain Z12 (Fig. 6B and C). The c-di-GMP contents in strain Z12 with adding GTP were also determined, and the results showed that the addition of GTP could significantly ($P < 0.01$) increase the content of c-di-GMP in strain Z12 (Fig. 6D). The effect of GTP on expression levels of MSHA type IV pili genes was determined, as shown in Fig. 6E. The MSHA type IV pili genes were significantly upregulated with the addition of GTP both in strains Z12 and Z12Δ*luxS*, suggesting that GTP can promote the expression of MSHA type IV pili genes. Accordingly, an increase of c-di-GMP by addition of GTP promotes the expression level of MSHA type IV pili genes.

C-di-GMP contributes to the adhesion of *A. veronii*

Despite the promotion effect of c-di-GMP on the expression of MSHA type IV pili genes, the effect of c-di-GMP on adhesion of *A. veronii* remains to be elucidated. As shown in Fig. 7A, based on fluorescence microscopy observation, it was found that there were more FITC-labeled bacterial cells of strain Z12 attached to the surface of erythrocytes, while fewer FITC-labeled bacterial cells of strain Z12Δ*luxS* adhered to erythrocytes. The addition of GTP could significantly promote the adhesion of strain Z12Δ*luxS* to the surface of erythrocytes. The number of FITC-labeled bacterial cells adhering to each erythrocyte was also determined, and the average number of Z12Δ*luxS* cells adhering to each erythrocyte was significantly lower than that of strain Z12, as well as strain Z12Δ*luxS* with adding GTP (Fig. 7B). The adhesion percentages to erythrocytes of strains Z12 and Z12Δ*luxS* with adding GTP were significantly ($P < 0.01$) higher than that of strain Z12Δ*luxS* (Fig. 7C). Based on these results, we conclude that increase of c-di-GMP by addition of GTP can contribute to adherence of *A. veronii* to erythrocytes.

DISCUSSION

A. veronii is a common pathogen of zoonosis, which can colonize the gastrointestinal tract of the host, thus causing severe *Aeromonas* gastroenteritis. Colonization is the main means for pathogens to infect the host, and the adhesion ability of pathogens determines whether they can successfully colonize the host. In this study, we propose a regulation mechanism for adhesion of *A. veronii* by AI-2 through mediating by c-di-GMP, which will contribute to increasing the understanding of colonization strategy of pathogens.

Quorum sensing (QS), a bacterial cell-to-cell communication depending on production and response of signaling molecules called autoinducers, has been evidenced to be widely involved in the regulation of various physiological functions of bacteria including luminescence (21), motility (22), biofilm (23), toxin production (24), and so on. LuxS/AI-2 QS system, which is mediated by AI-2 produced by LuxS as autoinducer, plays an important role in regulating gene expression in multiple Gram-positive and Gram-negative bacteria. The genome sequences of *Aeromonas* species have shown the presence of gene *luxS* encoding LuxS protein for synthesis of AI-2, and the *luxS* mutant of *A. hydrophila* SSU exhibited decreased motility and increased virulence, as well as increase of biofilm (25). Despite there have been reports on AI-2 regulating the

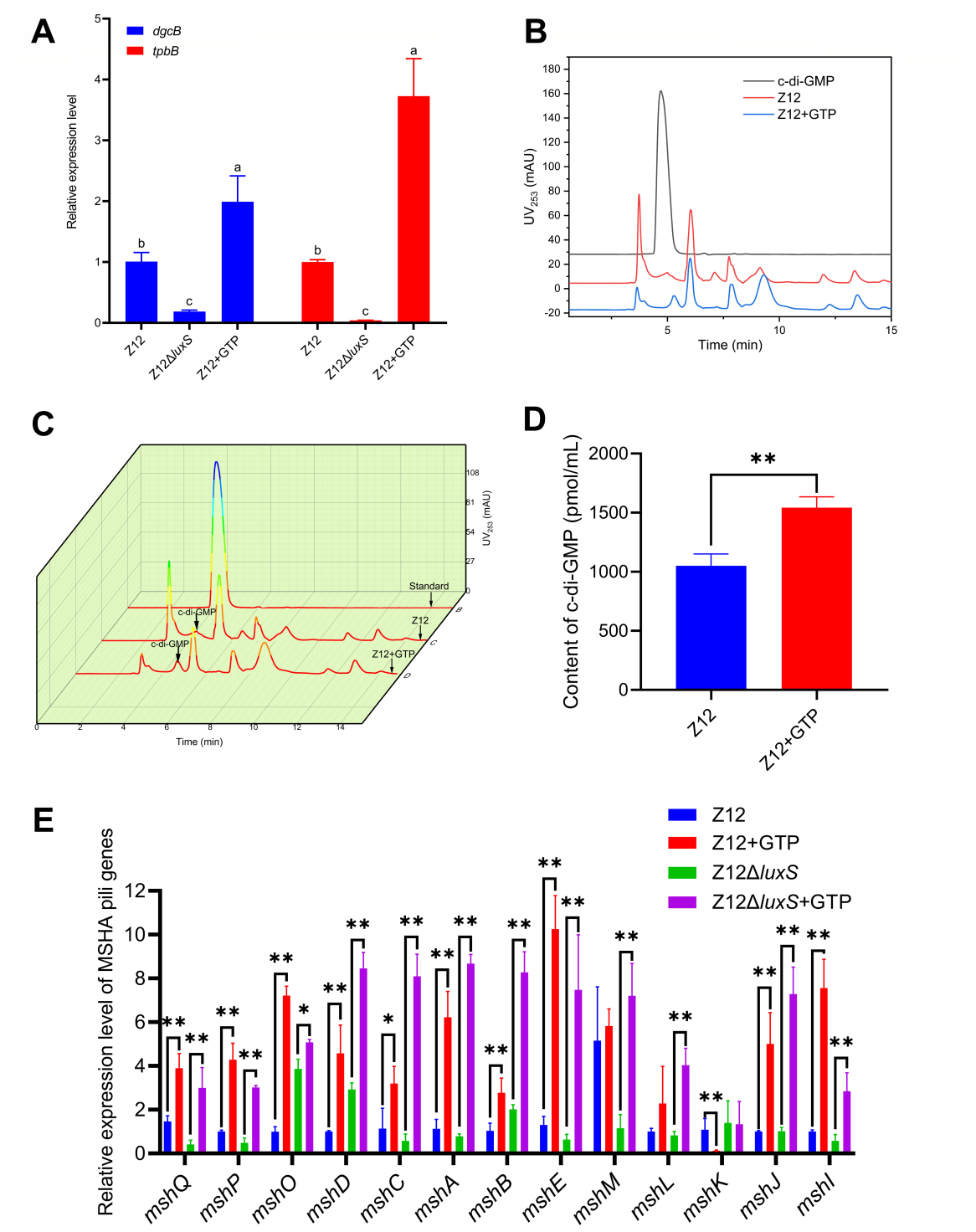

FIG 6 The effect of c-di-GMP on expression of MSHA type IV pili genes. (A) The relative expression levels of *dgcB* and *tpbB*. (B) HPLC spectra of c-di-GMP in strain Z12 with or without adding 1 mM of GTP. (C) HPLC 3D spectra of c-di-GMP in strain Z12 with or without adding 1 mM of GTP. (D) The contents of c-di-GMP in strain Z12 with or without adding 1 mM of GTP. (E) The relative expression level of MSHA pili genes in strains Z12 and Z12Δ*luxS* with or without adding 1 mM of GTP. Data are presented as mean ± SD. * represents a statistically significant difference of $P < 0.05$. ** represents a statistically significant difference of $P < 0.01$.

physiological function of *Aeromonas* sp., the regulatory effect of AI-2 on adhesion of *Aeromonas* sp. is still unclear. We demonstrated that the mutation of *luxS* in *A. veronii* Z12 can significantly lower its adhesion ability to erythrocytes and intestinal mucus of the

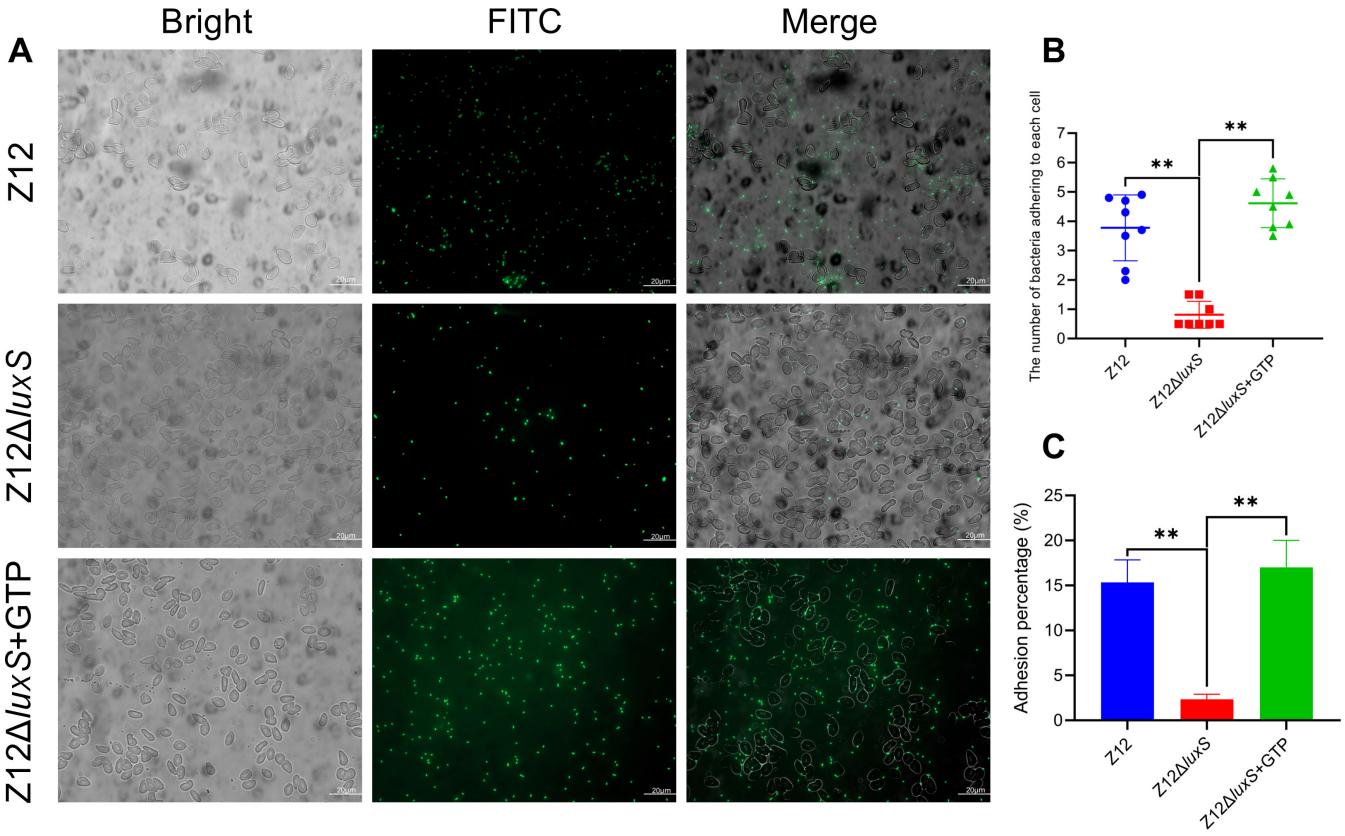

FIG 7 The effect of c-di-GMP on adherence. (A) The adherence of FITC-labeled bacterial cells to erythrocytes. Scale bars represent 20 µm. (B) The number of bacterial cells adhering to each erythrocyte. (C) Adhesion percentage of strains Z12, Z12Δ*luxS*, and Z12Δ*luxS* with adding 1 mM of GTP. Data are presented as mean ± SD. ** represents a statistically significant difference of $P < 0.01$.

loach, and complement of AI-2 will increase the adhesion ability of the mutation strain, which indicated that AI-2 can positively regulate adhesion ability of *A. veronii*. Adhesion is closely related to the formation of biofilm, which depends on bacteria adhering to the biotic or abiotic surface (26). The positive regulation of AI-2 on adhesion will promote the formation of biofilm in *A. veronii*, and McNab et al. also evidenced that the *luxS* mutation strain of *Streptococcus gordonii* was unable to form a mixed species biofilm (27), but this result is inconsistent with the report that AI-2 negatively regulated the formation of biofilm in *A. hydrophila* SSU (25). Kozlova et al. further investigated the effect of c-di-GMP on the biofilm of *A. hydrophila* SSU, which showed that c-di-GMP overproduction dramatically enhanced biofilm formation (28), the negative regulation of AI-2 on biofilm formation of *A. hydrophila* SSU may be mediated by c-di-GMP.

Previous research has demonstrated that HapR, a major regulator of QS in *Vibrio cholerae*, can reduce the levels of c-di-GMP (12). We also measured the content of c-di-GMP between wild strain Z12 and mutation strain Z12Δ*luxS*, the results showed that the deficiency of AI-2 lowers the content of c-di-GMP. Meanwhile, the expression level of *hapR* was upregulated in the mutation strain Z12Δ*luxS*. These results are consistent with what reported by Waters et al. that the high expression of *hapR* encoding HapR protein limits the synthesis of c-di-GMP (12). High expression of *hapR* in the AI-2 deficient strain is uncommon, because the low concentration of AI-2 in the mutant strain Z12Δ*luxS* leads to phosphorylation of LuxO (29), which activates expression of Qrr sRNAs (19), thereby promoting translation of the mRNA encoding AphA, a master regulator of QS at low-cell density, and inhibiting translation of the mRNA encoding HapR, a master regulator of QS at high-cell density. The relative expression levels of *luxO*, *hfq* (genes 0184 and 0889), and *aphA* between strains Z12 and Z12Δ*luxS* were determined, which

showed that these genes were significantly ($P < 0.01$) upregulated in strain Z12Δ*luxS* compared with strain Z12 (Fig. S3), the expression trend of these genes in *Aeromonas* is consistent with their expression in *Vibrio harveyi* (30) and *Vibrio cholerae* (31), suggesting that the high expression level of *hapR* in strain Z12Δ*luxS* may be due to the presence of other regulatory pathways, rather than experimental issues. In fact, there exists other regulatory pathways for *hapR* expression, which reported by Weber et al. that the sigma factor RpoS could significantly promote the expression of *vanT* mRNA, which encodes a LuxR homolog in *V. anguillarum* (20). The *rpoS* expression was upregulated in strain Z12Δ*luxS*, and further stabilized *hapR* mRNA and induced HapR expression. Therefore, it explains the possible reason for the upregulation of *hapR* in the AI-2 deficient strain Z12Δ*luxS*.

Cyclic-di-GMP, a ubiquitous second messenger in bacteria, is generated by DGC-containing GGDEF domains and degraded by phosphodiesterase (PDE) containing EAL or HD-GYP domains. Evidence of the regulation of motility and biofilm by c-di-GMP has been reported in *Aeromonas*, which showed that the overexpression of AdrA-containing GGDEF domain increased biofilm and decreased motility in *A. veronii* (11). The c-di-GMP signaling network not only relies on its content regulated by DGC and PDE, but also on the receptors for binding c-di-GMP. Proteins containing PilZ domain were the earliest discovered c-di-GMP receptors (32), and the annotation of genome sequence of *A. veronii* Z12 showed that the type IV pilus assembly proteins encoded by *pilZ* were identified as PilZ domain that contains a classic c-di-GMP binding domain. However, the decline of c-di-GMP caused by AI-2 deficiency did not result in a change in *pilZ* expression level; therefore, there existed other c-di-GMP receptors mediated by c-di-GMP in *A. veronii* Z12. We further demonstrated MshE encoded by *mshE* is a potential c-di-GMP receptor in *A. veronii* Z12, and the expression of *mshE* is regulated by c-di-GMP. MshE has been previously reported to contribute to binding c-di-GMP in *Vibrio cholerae*, c-di-GMP can interact with the Arg9 residue of MshE (33) and promote the formation of MSHA pili (17). In *A. veronii*, MSHA pili have been identified by Hadi et al. as a crucial contributor to adherence, which contain two promoters, that are responsible for the expression of *mshIJKLMNEGF* and *mshBACDOPQ* in *A. veronii* (10). Additionally, the strength of the upstream promoter of *mshB* is significantly higher than that of the upstream promoter of *mshI*, and this identification is consistent with our results that the transcription level of *mshODBG* downstream of *mshB* is significantly higher than that of downstream genes with *mshI* as the promoter (10), but *mshG* is an exception. Meanwhile, we found that the transcriptional levels of different genes in the same gene cluster are different, which may be caused by the following reasons. First of all, while the promoter upstream of the operon gene controls the start of transcription, theoretically it will form a continuous mRNA, but the early research has demonstrated that the gene expression inside the operon is uneven (34), and it was found that the expression level of the continuous genes inside the operon decreases successively, that is, the operon decays (35), which is consistent with our results, where the transcription level of *mshBACDOPQ* shows a decreasing trend in sequence, except for *mshD* and *mshO*. Second, there may exist internal promoters in the gene cluster that play a crucial role in regulating gene expression in the same gene cluster, even leading to inconsistent changes in different genes in the same gene cluster (36). Accordingly, we speculate that there may still be internal promoters that have not been identified yet in the MSHA family gene clusters of *A. veronii*, which cause the inconsistency of the different gene expression in the same gene cluster.

MshE is the ATPase that supplies energy for the formation and secretion of MSHA pili, MshA export and the function of the pili in adherence depend on c-di-GMP binding to MshE (33), and c-di-GMP binding to MshE can regulate MSHA pilus extension and retraction dynamics, thus modulating surface attachment and colonization of *V. cholerae* (16). Therefore, the low concentration of c-di-GMP in strain Z12Δ*luxS* affects the *mshE* expression and functions of MshE, finally limiting the formation of MSHA type IV pili. The addition of GTP promotes the expression of genes encoding proteins containing GGDEF

domain and increases the content of c-di-GMP, which further causes the upregulated expression of MSHA genes and increases the adherence to host cells. The MSHA type IV pili system is one of the most important adherence systems in *Aeromonas*, which is essential to adhesion, biofilm formation, and colonization (37), and the expression of the MSHA pilus can be regulated by environmental factors which reported by Kirov and Sanderson that *A. veronii* increases its MSHA pilus expression under 22°C in liquid culture (9). Our research provides an AI-2 regulated MSHA type IV expression model mediated by c-di-GMP in *A. veronii*, which further confirms that the pili formation of *A. veronii* is required for *A. veronii* adherence to host cells. Although many adherence studies have confirmed that multiple adherence systems, including OMPs (38), LPS (39), and pili (40), exist in *Aeromonas*, our study found that AI-2 only regulates pili formation in *A. veronii* Z12, instead of OMPs and LPS. This adherence mechanism regulated by AI-2 through mediating by c-di-GMP may exist in other pathogens, which is worth paying more attention in the future research.

The present research explored, for the first time, the adherence mechanism of *A. veronii* regulated by AI-2, which reveals a role for AI-2 in the regulation of MSHA type IV pili expression mediated by c-di-GMP, the downregulated expression of MSHA type IV pili genes in strain Z12Δ*luxS* reduced the adhesion ability. AI-2, that regulates adherence mediated by c-di-GMP, can play an essential role in regulating adherence of other pathogens, and this study can provide a better understanding of *A. veronii* adherence and its colonization strategy.

MATERIALS AND METHODS

Bacterial strains and growth conditions

Strains and plasmids are described in Table 1. *A. veronii* Z12 (MN922947) was cultured in Luria-Bertani medium (LB, the distilled water containing 1% tryptone, 0.5% yeast extract, and 1% NaCl, pH 7.2–7.6) at 30°C. *V. harveyi* BB170, used as the reporter strain to measure the AI-2 activity, was cultured in AB medium (41) at 30°C. *Escherichia coli* BL21 (DE3), used for recombinant plasmids expression, was cultured in LB medium at 37°C. *E. coli* S17-1 λpir, used as donor strain for conjugal transfer, was cultured in LB medium at 37°C.

Construction of AI-2 deficient strain and complement

The schematic representation for deleting the *luxS* gene, which encoded the LuxS enzyme representing the last enzymatic step of AI-2 synthesis (Fig. 1A), was shown

TABLE 1 Strains and plasmids used in this study

Strains and plasmids	Relevant description
Strains	
Z12	*Aeromonas veronii* wild-type strain
Z12Δ*luxS*	The *luxS* gene deletion mutant of *Aeromonas veronii* Z12
E. coli S17-1 λpir	*thi pro hsdR hsdM*$^{+}$*recA* RP4–2-Tc::Mu-Km::Tn7
pRE112Δ*luxS*-S17-1 λpir	*E. coli* S17-1 λpir transformed with pRE112Δ*luxS*
E. coli BL21(DE3)	Expression host
Strain B-pET28a-*mshE*	*E. coli* BL21(DE3) transformed with pET28a-*mshE*
Vibrio harveyi BB170	The reporter strain for measuring the autoinducer-2 activity
Plasmids	
pRE112	pGP704 suicide plasmid, pir dependent, oriT, oriV, sacB, Cmr
pRE112Δ*luxS*	pRE112 derivative containing the *luxS* gene upstream and downstream of the frame, Cmr
pET28a	Expression vector with kanamycin resistance and BamHI/Xho I sites at 158–203
pET28a-*mshE*	pET28a containing the *mshE* gene

in Fig. 1B. The upstream and downstream of the *luxS* gene were amplified using PCR with pairs of primers F3, R3 and F4, R4, then ligated through overlap extension PCR. The purified enzyme-digested ligation products (KpnI/NdeI sites) were used to ligate with KpnI/NdeI-digested pRE112 to construct the plasmid pRE112Δ*luxS*. After that, the plasmid pRE112Δ*luxS* was transformed into *E. coli* S17-1 λpir, which was further used to construct the AI-2 deficient strain Z12Δ*luxS* through conjugal transfer of the plasmid pRE112Δ*luxS* into *A. veronii* Z12 on the LB plate by adding 100 µg/mL of ampicillin and 30 µg/mL of chloramphenicol. The strain Z12Δ*luxS* was confirmed by PCR amplification with primer pairs of F1, R1 and F2, *R2*. The complement of AI-2 was performed by adding exogenous AI-2 (300 µM), which was synthesized by incubation with proteins Pfs and LuxS, together with 1 mM S-adenosyl-homocysteine (Sigma, USA) as substrate, in 10 mM sodium phosphate buffer at 37°C for 5 h, according to our previous research (42).

Detection of AI-2 activity and bacterial growth

V. harveyi BB170 was inoculated into 5 mL of AB medium at 30°C for 16 h, then diluted 1:5,000 in fresh AB medium. The Z12 cell-free culture, Z12Δ*luxS* cell-free culture, and Z12Δ*luxS* cell-free culture with adding the synthesized AI-2 were inoculated into the diluted BB170 culture at a ratio of 1:9, respectively. The same concentration of BB170 cell-free culture was inoculated into the diluted BB170 culture as the positive control, and the same concentration of LB and AB medium was added to the diluted BB170 culture as the negative control, respectively. All the groups were cultured at 30°C, and the luminescence values in different groups were measured by multi-mode microplate detection system (PerkinElmer, USA) every 0.5 h, until the lowest luminescence values were detected.

The growth conditions of strains Z12, Z12Δ*luxS*, and Z12Δ*luxS* with AI-2 were measured by automatic growth curve analyzer (Oy Growth Curves Ab Ltd., Finland) at the optical density of 600 nm every 1 h.

Adhesion ability to erythrocytes

Blood was harvested from the tail vein of the loach (*Paramisgurnus dabryanus*) using a sterile syringe. The obtained blood was added gently to a 2 mL centrifuge tube containing 0.1 mg/mL heparin sodium solution. After that, erythrocytes were obtained from the blood by centrifugation of 1,300 rpm at 4°C for 30 min, which were further washed three times with 0.7% physiological saline, and finally resuspended in 0.7% saline buffer to be used. Bacterial cells of strains Z12, Z12Δ*luxS*, and Z12Δ*luxS* with AI-2 were harvested by centrifugation at 12,000 rpm for 5 min, and then bacterial cells were labeled by 10 µL of fluorescein 5-isothiocyanate (FITC, 1 mg/mL) (Sigma, USA) at room temperature for 30 min. The redundant FITC were washed off by phosphate-buffered saline (PBS) for three times. The FITC-labeled bacterial cells of strains Z12, Z12Δ*luxS*, and Z12Δ*luxS* with AI-2 were resuspended in PBS with the same concentration, and mixed with erythrocytes, respectively. After gentle shaking for 30 min, 20 µL of mixtures was added on the slide and observed under fluorescence microscope (Olympus, Japan) to measure the adhesion ability. The effect of GTP on adhesion ability of strain Z12Δ*luxS* to erythrocytes was also determined. The bacterial cells of strains Z12, Z12Δ*luxS*, and Z12Δ*luxS* with 1 mM GTP were harvested and labeled by FITC, then measured the adhesion ability according to the above method.

Scanning electron microscopy analysis

After incubating bacterial cells with erythrocytes at room temperature for 30 min, erythrocytes were harvested by centrifugation of 1,300 rpm at 4°C for 30 min, and washed with 0.1 M of PBS for three times to remove non-adhesive bacterial cells. The erythrocytes were fixed by 2.5% glutaraldehyde at 4°C for 24 hr, and then cleared out glutaraldehyde by centrifugation of 1,300 rpm at 4°C for 30 min. After that, erythrocytes were gradient dehydration with 30–100% ethanol for 20 min per gradient. Subsequently,

the samples were dropped onto the sample stage of the double-sided conductive tape, respectively, and sprayed with the ion sputter instrument (Hitachi, Japan), then observed using the scanning electron microscope (Jeol, Japan) to evaluate the adhesion ability.

Adhesion ability to intestinal mucus

After anesthesia of the loach (*P. dabryanus*) by 3-Aminobenzoic acid ethyl ester methanesulfonate (MS-222, 100 mg/L), intestinal tissue was harvested in a sterile environment, and cutoff about 1 cm at both ends, evenly cut into three sections including front, middle, and back, then cut open. About 10 mM PBS (pH 7.4) was used to wash the intestinal tissue, after which intestinal mucus was gently scraped off. The harvested mucus was added with same volume of PBS, and measured the protein contents inside by NanoDrop (Thermo, USA). After adjusting the concentration of mucus to 10 mg/mL, 100 µL of the mucus and bovine serum albumin (BSA) as negative control was added into a 96-well ELISA plate, respectively, and incubated overnight at 4°C. After that, the FITC-labeled bacterial cells of strains Z12 and Z12Δ*luxS* were added into the mucus and BSA, respectively, and incubated at room temperature for 3 h, after which washed with PBS for three times, and resuspended in 200 µL of PBS. The adhesion ability to intestinal mucus was determined by fluorescence microscope (Olympus, Japan) and multifunctional enzyme-linked immunosorbent assay (BioTek, USA).

Measurement of OMPs and LPS

After cultivation to the same growth period of strains Z12 and Z12Δ*luxS*, bacterial cells were harvested by centrifugation at 12,000 rpm for 10 min, and washed with PBS for three times. After that, bacterial OMPs were extracted by bacterial outer membrane protein extraction kit (Bestbio, China), and further measured by BSA method. Bacterial LPS was extracted and measured by LPS ELISA kit (JingMei Bio, China).

Transmission electron microscopy analysis

About 1 mL of overnight static grown bacterial cultures of strains Z12 and Z12Δ*luxS* was centrifuged for 10 min at 4,000 rpm to harvest bacterial cells, and washed with PBS for three times. About 50 µL of bacterial cells was dropped on the copper mesh and kept at room temperature for 15 min, then the copper mesh was suspended in 2% tungsten phosphate. Finally, pili of strains Z12 and Z12Δ*luxS* were observed under transmission electron microscope (Jeol, Japan).

Determination of c-di-GMP

After cultivation to the same growth period of strains Z12 and Z12Δ*luxS*, bacterial cells were harvested by centrifugation at 12,000 rpm for 10 min, and washed with PBS for three times. After that, bacterial cells were inoculated into 1 mL of extracting solution (acetonitrile:water = 4:1, vol/vol), and placed in a 100°C water bath for 10 min. Then, the extracts were quickly put into an ice-water mixture to cool for 10 min, and further harvested by centrifugation at 12,000 rpm for 10 min. The above extraction steps were repeated three times, three times of extraction solutions were mixed for detection. C-di-GMP contents of strains Z12 and Z12Δ*luxS* were determined by HPLC, which was carried out using a C18 chromatographic column (4.6 mm × 150 mm, 5 µm) with a mobile phase of methanol:water = 4:1 (vol/vol) and detection wavelength of 254 nm. Gradient diluted c-di-GMP (Sigma, USA) standard is used to plot the standard curve of absorption peak height and concentration, then c-di-GMP contents in extraction solutions of strains Z12 and Z12Δ*luxS* were measured. The effect of GTP on the c-di-GMP contents in strain Z12 was also determined, according to the above method. The extraction solutions of strains Z12 and Z2 with adding 1 mM of GTP were used to determine the c-di-GMP contents.

Real-time RT-PCR analysis

Bacterial cells were harvested by centrifugation of 12,000 rpm at 4°C for 10 min after bacterial cultures reached the same level that the optical density at 600 nm was between 0.8 and 1.0. The harvested bacterial cells were washed with PBS for three times, which were further used to isolate RNA based on RNAprep Pure Cell/Bacteria Kit (TIANGEN, China). Equal amounts of qualified total RNA with integrity and appropriate concentration were used to generate cDNA based on M5 HiPer First Strand cDNA Synthesis Kit (Mei5bio, China). Real-time PCR was carried out using lightCycler 480 II fluorescence quantitative PCR instrument (Roche, Switzerland) based on 2 × SYBR Premix UrTaq II kit (Nobelab, China). The primer pairs in this study for RT-PCR are listed in Table S2; 16S rRNA was used as a reference gene to normalize the expression changes. The relative gene expressions were quantified using the $2^{-\Delta\Delta Ct}$ method (43).

Expression of protein MshE

The primers of *mshE* gene containing BamHI and XhoI sites are listed in Table S2, which were used to amplify *mshE* gene using PCR. The PCR products were digested by BamHI and XhoI, then the purified enzyme-digested products were ligated with BamHI/Xho I-digested pET28a by M5 HiPer T4 DNA Ligase (Nobelab, China) to construct the recombinant expression vector pET28a-*mshE*. The recombinant expression vector was transformed to the expression strain *E. coli* BL21 (DE3) and cultured on LB plates containing 50 µg/mL of kanamycin at 37°C overnight. The identified colonies containing recombinant plasmid were inoculated into LB medium containing kanamycin, after which 0.5 mM isopropyl-β-D-thiogalactopyranoside (IPTG) was added when the optical density at 600 nm was 0.4. After IPTG induction for 48 h, bacterial cells were harvested by centrifugation at 12,000 rpm for 40 min, and washed with PBS for three times. About 500 µL of harvested bacterial cells was lysed and centrifuged to obtain intracellular supernatant, which was further used to analyze the expression levels of MshE with SDS-PAGE. After that, the resultant intracellular supernatant was added into affinity chromatography column (Sangon, China) with low-speed oscillation for 1 h at 4°C, and purified using a flow rate of 0.5–1.0 mL/min. The effluent was collected and used to remove miscellaneous proteins with 50 mL of washing buffer, as well as harvesting target protein with 10 mL of elute buffer. The purified protein MshE was dialyzed with ultrapure water at 4°C and the protein concentration was adjusted to 2 mM for subsequent experiments.

Circular dichroism spectra

The circular dichroism (CD) spectra of c-di-GMP and MshE were carried out on a CD spectrometer (Applied Photophysics, UK).About 0.25 mM of MshE was mixed with different concentrations of c-di-GMP including 90, 180, 270, and 450 pm. Samples were scanned three times in the region from 205 to 300 nm with ultrapure water as blank control, and the average values of spectral data were used to plot the CD spectra.

Statistical analyses

The statistical significance of the difference between different groups was analyzed using Student' s *t* test, *P* value of less than 0.05 was considered statistically significant. The CD spectra and c-di-GMP spectra were plotted by OriginPro 2021, and other figures were plotted by GraphPad Prism 8.0.2.

ACKNOWLEDGMENTS

This work is supported by the National Natural Science Foundation of China (32000073), the Key Scientific Research Programs of Henan Education Department (21A180011), and the Guangdong Basic and Applied Basic Research Foundation (2020B1515120012).

AUTHOR AFFILIATIONS

[1]College of Life Sciences, Henan Normal University, Xinxiang, China
[2]Henan Province Engineering Laboratory for Bioconversion Technology of Functional Microbes, Xinxiang, China
[3]Advanced Environmental Biotechnology Center, Nanyang Environment and Water Research Institute, Nanyang Technological University, Singapore, Singapore

AUTHOR ORCIDs

Xiaohua Xia http://orcid.org/0000-0001-5357-0048
Hailei Wang http://orcid.org/0009-0006-0073-6319

FUNDING

Funder	Grant(s)	Author(s)
The National Natural Science Foundation of China	32000073	Yi Li
The Key Scientific Research Programs of Henan Education Department	21A180011	Yi Li

AUTHOR CONTRIBUTIONS

Yi Li, Data curation, Funding acquisition, Methodology, Writing – original draft | Shuo Han, Data curation, Investigation, Methodology, Software | Yuqi Wang, Data curation, Investigation | Mengyuan Qin, Formal analysis, Investigation, Software | Chengjin Lu, Data curation, Investigation, Software | Yingke Ma, Data curation, Software, Validation | Wenqing Yang, Data curation, Software | Jiajia Liu, Data curation, Formal analysis | Xiaohua Xia, Formal analysis, Supervision, Validation | Hailei Wang, Data curation, Investigation, Supervision, Writing – review and editing

ADDITIONAL FILES

The following material is available online.

Supplemental Material

Fig. S1 to S3, Tables S1 to S2 (AEM00819-23-s0001.docx). Fig. S1-Adherence of *A. veronii* to intestinal mucus. Fig. S2-Schematic representation of the synthesis of c-di-GMP. Fig. S3-The relative expression levels of *luxO*, *hfq* (gene 0184 and gene 0889), and *aphA*. Table S1-The pili gene families. Table S2-Primers used in this study.

REFERENCES

1. Khajanchi BK, Fadl AA, Borchardt MA, Berg RL, Horneman AJ, Stemper ME, Joseph SW, Moyer NP, Sha J, Chopra AK. 2010. Distribution of virulence factors and molecular fingerprinting of *Aeromonas* species isolates from water and clinical samples: suggestive evidence of water-to-human transmission. Appl Environ Microbiol 76:2313–2325. https://doi.org/10.1128/AEM.02535-09
2. Zhou Y, Yu L, Nan Z, Zhang P, Kan B, Yan D, Su J. 2019. Taxonomy, virulence genes and antimicrobial resistance of *Aeromonas* isolated from extra-intestinal and intestinal infections. BMC Infect Dis 19:158. https://doi.org/10.1186/s12879-019-3766-0
3. Parker JL, Shaw JG. 2011. *Aeromonas* spp. clinical microbiology and disease. J Infect 62:109–118. https://doi.org/10.1016/j.jinf.2010.12.003
4. Hickman-Brenner FW, MacDonald KL, Steigerwalt AG, Fanning GR, Brenner DJ, Farmer JJ. 1987. *Aeromonas veronii*, a new ornithine decarboxylase-positive species that may cause diarrhea. J Clin Microbiol 25:900–906. https://doi.org/10.1128/jcm.25.5.900-906.1987
5. Li X, Song H, Wang J, Zhang D, Shan X, Yang B, Kang Y, Qian A, Zhang L, Sun W. 2021. Functional analysis of *fis* in *Aeromonas veronii* TH0426 reveals a key role in the regulation of virulence. Microb Pathog 159:105123. https://doi.org/10.1016/j.micpath.2021.105123
6. Anderson BN, Ding AM, Nilsson LM, Kusuma K, Tchesnokova V, Vogel V, Sokurenko EV, Thomas WE. 2007. Weak rolling adhesion enhances bacterial surface colonization. J Bacteriol 189:1794–1802. https://doi.org/10.1128/JB.00899-06
7. Vázquez-Juárez RC, Barrera-Saldaña HA, Hernández-Saavedra NY, Gómez-Chiarri M, Ascencio F. 2003. Molecular cloning, sequencing and characterization of *omp48*, the gene encoding for an antigenic outer membrane protein from *Aeromonas veronii*. J Appl Microbiol 94:908–918. https://doi.org/10.1046/j.1365-2672.2003.01928.x
8. Merino S, Camprubí S, Tomás JM. 1992. Effect of growth temperature on outer membrane components and virulence of *Aeromonas hydrophila* strains of serotype O:34. Infect Immun 60:4343–4349. https://doi.org/10.1128/iai.60.10.4343-4349.1992
9. Kirov SM, Sanderson K. 1996. Characterization of a type IV bundle-forming pilus (SFP) from a gastroenteritis-associated strain of *Aeromonas veronii* biovar sobria. Microb Pathog 21:23–34. https://doi.org/10.1006/mpat.1996.0039

10. Hadi N, Yang Q, Barnett TC, Tabei SMB, Kirov SM, Shaw JG. 2012. Bundle-forming pilus locus of *Aeromonas veronii* bv. Infect Immun 80:1351–1360. https://doi.org/10.1128/IAI.06304-11
11. Rahman M, Simm R, Kader A, Basseres E, Römling U, Möllby R. 2007. The role of c-di-GMP signaling in an *Aeromonas veronii* biovar sobria strain. FEMS Microbiol Lett 273:172–179. https://doi.org/10.1111/j.1574-6968.2007.00803.x
12. Waters CM, Lu W, Rabinowitz JD, Bassler BL. 2008. Quorum sensing controls biofilm formation in *Vibrio cholerae* through modulation of cyclic di-GMP levels and repression of *vpsT*. J Bacteriol 190:2527–2536. https://doi.org/10.1128/JB.01756-07
13. Sun J, Daniel R, Wagner-Döbler I, Zeng A-P. 2004. Is autoinducer-2 a universal signal for interspecies communication: a comparative genomic and phylogenetic analysis of the synthesis and signal transduction pathways. BMC Evol Biol 4:36. https://doi.org/10.1186/1471-2148-4-36
14. Ho AS, Mietzner TA, Smith AJ, Schoolnik GK. 1990. The pili of *Aeromonas hydrophila*: identification of an environmentally regulated "mini pilin". J Exp Med 172:795–806. https://doi.org/10.1084/jem.172.3.795
15. Li Y, Wu X, Han S, Chen Z, Qin M, Liu L, Jiang X, Wang H. 2022. The effect of N-acyl-homoserine lactones-mediated quorum sensing on intestinal colonization and damage by *Aeromonas veronii*. Aquaculture 561:738627. https://doi.org/10.1016/j.aquaculture.2022.738627
16. Floyd KA, Lee CK, Xian W, Nametalla M, Valentine A, Crair B, Zhu S, Hughes HQ, Chlebek JL, Wu DC, Hwan Park J, Farhat AM, Lomba CJ, Ellison CK, Brun YV, Campos-Gomez J, Dalia AB, Liu J, Biais N, Wong GCL, Yildiz FH. 2020. c-di-GMP modulates type IV MSHA pilus retraction and surface attachment in *Vibrio cholerae*. Nat Commun 11:1549. https://doi.org/10.1038/s41467-020-15331-8
17. Jones CJ, Utada A, Davis KR, Thongsomboon W, Zamorano Sanchez D, Banakar V, Cegelski L, Wong GCL, Yildiz FH, Parsek MR. 2015. c-di-GMP regulates motile to sessile transition by modulating MshA pili biogenesis and near-surface motility behavior in *Vibrio cholerae*. PLoS Pathog 11:e1005068. https://doi.org/10.1371/journal.ppat.1005068
18. Lenz DH, Mok KC, Lilley BN, Kulkarni RV, Wingreen NS, Bassler BL. 2004. The small RNA chaperone Hfq and multiple small RNAs control quorum sensing in *Vibrio harveyi* and *Vibrio cholerae*. Cell 118:69–82. https://doi.org/10.1016/j.cell.2004.06.009
19. Feng L, Rutherford ST, Papenfort K, Bagert JD, van Kessel JC, Tirrell DA, Wingreen NS, Bassler BL. 2015. A qrr noncoding RNA deploys four different regulatory mechanisms to optimize quorum-sensing dynamics. Cell 160:228–240. https://doi.org/10.1016/j.cell.2014.11.051
20. Weber B, Croxatto A, Chen C, Milton DL. 2008. RpoS induces expression of the *Vibrio anguillarum* quorum-sensing regulator VanT. Microbiology (Reading) 154:767–780. https://doi.org/10.1099/mic.0.2007/014167-0
21. Bassler BL, Greenberg EP, Stevens AM. 1997. Cross-species induction of luminescence in the quorum-sensing bacterium *Vibrio harveyi*. J Bacteriol 179:4043–4045. https://doi.org/10.1128/jb.179.12.4043-4045.1997
22. Bearson BL, Bearson SMD. 2008. The role of the QseC quorum-sensing sensor kinase in colonization and norepinephrine-enhanced motility of *Salmonella enterica* serovar Typhimurium. Microb Pathog 44:271–278. https://doi.org/10.1016/j.micpath.2007.10.001
23. Suntharalingam P, Cvitkovitch DG. 2005. Quorum sensing in streptococcal biofilm formation. Trends Microbiol 13:3–6. https://doi.org/10.1016/j.tim.2004.11.009
24. Chen J, McClane BA. 2012. Role of the Agr-like quorum-sensing system in regulating toxin production by *Clostridium perfringens* type B strains CN1793 and CN1795. Infect Immun 80:3008–3017. https://doi.org/10.1128/IAI.00438-12
25. Kozlova EV, Popov VL, Sha J, Foltz SM, Erova TE, Agar SL, Horneman AJ, Chopra AK. 2008. Mutation in the S-ribosylhomocysteinase (*luxS*) gene involved in quorum sensing affects biofilm formation and virulence in a clinical isolate of *Aeromonas hydrophila*. Microb Pathog 45:343–354. https://doi.org/10.1016/j.micpath.2008.08.007
26. Prigent-Combaret C, Brombacher E, Vidal O, Ambert A, Lejeune P, Landini P, Dorel C. 2001. Complex regulatory network controls initial adhesion and biofilm formation in *Escherichia coli* via regulation of the *csgD* gene. J Bacteriol 183:7213–7223. https://doi.org/10.1128/JB.183.24.7213-7223.2001
27. McNab R, Ford SK, El-Sabaeny A, Barbieri B, Cook GS, Lamont RJ. 2003. LuxS-based signaling in *Streptococcus gordonii*: autoinducer 2 controls carbohydrate metabolism and biofilm formation with *Porphyromonas gingivalis*. J Bacteriol 185:274–284. https://doi.org/10.1128/JB.185.1.274-284.2003
28. Kozlova EV, Khajanchi BK, Sha J, Chopra AK. 2011. Quorum sensing and c-di-GMP-dependent alterations in gene transcripts and virulence-associated phenotypes in a clinical isolate of *Aeromonas hydrophila*. Microb Pathog 50:213–223. https://doi.org/10.1016/j.micpath.2011.01.007
29. Freeman JA, Bassler BL. 1999. Sequence and function of LuxU: a two-component phosphorelay protein that regulates quorum sensing in *Vibrio harveyi*. J Bacteriol 181:899–906. https://doi.org/10.1128/JB.181.3.899-906.1999
30. Tu KC, Bassler BL. 2007. Multiple small RNAs act additively to integrate sensory information and control quorum sensing in *Vibrio harveyi*. Genes Dev 21:221–233. https://doi.org/10.1101/gad.1502407
31. Lin W, Kovacikova G, Skorupski K. 2007. The quorum sensing regulator HapR downregulates the expression of the virulence gene transcription factor AphA in *Vibrio cholerae* by antagonizing Lrp- and VpsR-mediated activation. Mol Microbiol 64:953–967. https://doi.org/10.1111/j.1365-2958.2007.05693.x
32. Amikam D, Galperin MY. 2006. PilZ domain is part of the bacterial c-di-GMP binding protein. Bioinformatics 22:3–6. https://doi.org/10.1093/bioinformatics/bti739
33. Roelofs KG, Jones CJ, Helman SR, Shang X, Orr MW, Goodson JR, Galperin MY, Yildiz FH, Lee VT. 2015. Systematic identification of cyclic-di-GMP binding proteins in *Vibrio cholerae* reveals a novel class of cyclic-di-GMP-binding ATPases associated with type II secretion systems. PLoS Pathog 11:e1005232. https://doi.org/10.1371/journal.ppat.1005232
34. Murakawa GJ, Kwan C, Yamashita J, Nierlich DP. 1991. Transcription and decay of the *lac* messenger: role of an intergenic terminator. J Bacteriol 173:28–36. https://doi.org/10.1128/jb.173.1.28-36.1991
35. Laing E, Mersinias V, Smith CP, Hubbard SJ. 2006. Analysis of gene expression in operons of *Streptomyces coelicolor*. Genome Biol 7:R46. https://doi.org/10.1186/gb-2006-7-6-r46
36. Gao Y-Z, Liu H, Chao H-J, Zhou N-Y, Parales RE. 2016. Constitutive expression of a nag-like dioxygenase gene through an internal promoter in the 2-chloronitrobenzene catabolism gene cluster of *Pseudomonas stutzeri* ZWLR2-1. Appl Environ Microbiol 82:3461–3470. https://doi.org/10.1128/AEM.00197-16
37. Watnick PI, Fullner KJ, Kolter R. 1999. A role for the mannose-sensitive hemagglutinin in biofilm formation by *Vibrio cholerae* El Tor. J Bacteriol 181:3606–3609. https://doi.org/10.1128/JB.181.11.3606-3609.1999
38. Rocha-DE-Souza CM, Colombo AV, Hirata R, Mattos-Guaraldi AL, Monteiro-Leal LH, Previato JO, Freitas AC, Andrade AFB. 2001. Identification of a 43-kDa outer-membrane protein as an adhesin in *Aeromonas caviae*. J Med Microbiol 50:313–319. https://doi.org/10.1099/0022-1317-50-4-313
39. Jimenez N, Canals R, Lacasta A, Kondakova AN, Lindner B, Knirel YA, Merino S, Regué M, Tomás JM. 2008. Molecular analysis of three *Aeromonas hydrophila* AH-3 (serotype O34) lipopolysaccharide core biosynthesis gene clusters. J Bacteriol 190:3176–3184. https://doi.org/10.1128/JB.01874-07
40. Hokama A, Honma Y, Nakasone N. 1990. Pili of an *Aeromonas hydrophila* strain as a possible colonization factor. Microbiol Immunol 34:901–915. https://doi.org/10.1111/j.1348-0421.1990.tb01069.x
41. Taga ME. 2005. Methods for analysis of bacterial autoinducer-2 production. Curr Protoc Microbiol Chapter 1:1C. https://doi.org/10.1002/9780471729259.mc01c01s00
42. Han S, Lu C, Qin M, Wang Y, Wu X, Xia X, Li Y. 2023. Alleviation effect of *Deinococcus* sp. Y35 together with autoinducer 2 on the physiological stress caused by *Microcystis aeruginosa* to zebrafish intestines. Aquaculture 576:739880. https://doi.org/10.1016/j.aquaculture.2023.739880
43. Livak KJ, Schmittgen TD. 2001. Analysis of relative gene expression data using real-time quantitative PCR and the $2^{-\Delta\Delta C_T}$ method. Methods 25:402–408. https://doi.org/10.1006/meth.2001.1262